Modern Physics Letters B, Vol. 15, No. 21 (2001) 895–903

A STUDY OF 2D ISING FERROMAGNETS WITH DIPOLE INTERACTIONS

M. IFTI*, Q. LI*, C. M. SOUKOULIS*,† and M. J. VELGAKIS‡,§

*Ames Laboratory and Department of Physics and Astronomy, Iowa State University, Ames, Iowa 50011, USA
†Research Center of Crete FORTH and Department of Physics, University of Crete, P. O. Box 1527, Heraklion 71110, Crete, Greece
‡Engineering Science Department, University of Patras, 26110 Patras, Greece
§velgakis@terpsi.iceht.forth.gr

Received 10 August 2001

A two-dimensional Ising model with competing short range ferromagnetic and long range dipolar interactions is used to study the transition properties and phase diagram in ultrathin magnetic films. Monte Carlo simulations in systems with exchange and dipolar interactions reveal a ground state of striped phases with varying width. By raising the temperature, the domain walls are smeared out by fluctuations, leading to a random domain mesoscopic phase with no long-range order, and finally the domains are melted to the high-temperature disordered phase. Local magnetic field distributions and specific heat calculations reproduced transition points consistent with the previous phase diagram of the model. The resemblance to the phase diagram in ultrathin magnetic films, such as in Fe/Cu(100), is discussed.

PACS Number(s): 42.55.Mv, 42.70.Hj, 78.90.+t

1. Introduction

The interplay between long-range dipole interactions and short-range exchange interactions can reveal interesting magnetic properties in complex systems. Such systems are usually characterized by an abundance of low-energy minima. The global minimum and consequently the true ground state has been an intriguing question in recent years. Extensively studied two-dimensional systems[1–4] concluded a series of striped phases with alternative stripes of up and down spins perpendicular to the plane, in a wide range of the exchange interactions. The motivation for these studies comes from the large number of experimental data available on the magnetic ordering observed in ferrimagnetic garnet films[7] and in ultrathin magnetic films such as Fe/Cu(100), Ni/Cu(001),[8] Co/Au(111), etc.

Ultrathin Fe films grown on a Cu(100) substrate have been widely studied, providing great insight into the magnetics and the structure in metal-on-metal films.

§Corresponding author.

Extensive experimental data indicated a dependence of the film structure and magnetic properties on the film thickness, the temperature, growth conditions, etc.[9] Specifically, a ferromagnetic fcc(100) Fe phase (or most likely a fct phase) is stabilized on a Cu(100) substrate up to some critical film thickness ($\sim$ 4–5 Fe monolayers) for either low or room temperature grown films. This phase is organized with the spins oriented perpendicularly to the film surface attributed to the prevailing of surface anisotropy. Thus, the ground state ordering is not the striped phase, as expected. For low temperature grown Fe films (about 100 K), above this critical thickness, the film fcc(100) structure is transformed into a bcc(110) structure resulting gradually in the spins reorientation from perpendicular to in-plane, which is believed to be primarily due to the reduction of magnetic anisotropy and gain of shape anisotropy. On the other hand, for room temperature grown Fe films (about 300 K), the perpendicular magnetization persists up to $\sim$10–11 Fe monolayers, when spin reorientation from perpendicular to in-plane occurs with the onset of the bcc(110) phase. Before this reorientation takes place, a third phase is observed in the thickness range $\sim$4–10 monolayers, which consists of an antiferromagnetic fcc(100) Fe phase in the interior of the film and a ferromagnetic fcc(100) surface layer. Similar phase behaviour has been observed in other magnetic thin films, as in Co/Au(111).[10] Our interest here is focused on the temperature-dependence of the phase diagram in thin films, while studies on the thickness profile will be reported elsewhere.

2. Results and Discussion

The model we consider is a two-dimensional Ising system with short-range exchange interactions and long-range dipolar interactions in zero magnetic field, governed by the Hamiltonian,

$$H = -J \sum_{\langle i,j \rangle} S_i S_j + g \sum_{i,j} \frac{S_i S_j}{r_{ij}^3}\,, \tag{1}$$

on a square lattice $L \times L$ with periodic boundary conditions and the spins $S = \pm 1$ oriented perpendicularly to the plane, where the first summation is taken over nearest-neighbor pairs, while the second is extended to all pairs on the lattice. The constants J and g (both positive) represent the exchange interaction and the dipolar interaction, respectively. This Hamiltonian can describe the interaction of a uniaxial spin system in ultrathin magnetic films on a nonmagnetic substrate.[1–6] The ground state properties of this model seems to be well established. The competitive play between the short-range exchange interactions, which favour the ferromagnetic phase, and the long-range dipole interactions, which favour the antiferromagnetic phase, are responsible for the observed variety of phases. The possible ground states include antiferromagnetic (AF), ferromagnetic (FM), striped, and checkerboard phases. As far as the ladder phase is concerned, it has been argued that its ground energy is very close to the striped phase, but not lower. However, we were able to observe only the first three phases by varying the exchange coupling J/g.

In agreement with previous work,[5] we find that for $J/g < 0.854$ the ground state of this system is an AF phase, while for $J/g > 0.854$ the ground state is the striped phase with up and down spins forming alternating stripes with a width h depending strongly on the exchange coupling J/g. Actually, the stripe width h increases with the ratio J/g. For large $J/g \gg 1$ the ground state seemingly becomes ferromagnetic, although it has been argued[5] that the FM phase is unstable for any finite value of J/g for 2D spin systems due to the long-range character of the dipolar interactions. However, this argument is not unassailable. As mentioned before, since the width h increases with the ratio J/g, eventually in the limit case $J/g \to \infty$, an FM state is expected to be stabilized below T_C. While in the opposite case $J = 0$, an AF state is expected to be stabilized below T_N with the nearest neighboring spins aligned in opposite directions. In this study we concentrate on the striped ground state and in particular we focus on the phase diagram of the model. In our numerical calculations we have chosen such values for the exchange coupling J/g to yield a periodicity in the ground state which is commensurate with the size of the lattice we use.

At finite temperatures, the striped phase is perturbed by fluctuations and topological defects.[6,11–14] As the temperature is raised from zero, the system evolves through a two-step melting process to disordering; first a breakdown of the striped pattern and formation of extended domains at a transition temperature T_{C2}, followed by a transition to the paramagnetic phase at a higher transition temperature T_{C1}. The intermediate phase is also referred to by different authors as the floating solid or tetragonal liquid phase. Both transition points lie below the Curie temperature of the corresponding Ising ferromagnet. The intermediate state appears to be highly frustrated. Below T_{C1}, incommensurate phases are formed without long-range order[11] with a wave vector $k \sim \pi g/J$ and a period $l \sim 2\pi/k = 2J/g$. The spin structure is not stable because the domain walls fluctuate continuously, resulting in sort-range order. This melting process is consistent with the low temperature configurations of Fig. 1 calculated for $J/g = 8.9$, which corresponds to a striped ground state. We notice that as the temperature is raised, the fluctuations of the domain walls increase up to the temperature $T/g \cong 5$. Above this temperature the striped phase breaks down into configurations of extended domains of highly ordered spins, consequently the directional and translational symmetries associated with the striped phase are lost.

We investigated the spin ordering process of the model by closely examining numerically the specific heat curves. A number of Monte Carlo simulations were carried out on a 64×64 lattice. The specific heat dependence on the temperature is shown in Fig. 2 for $J/g = 8.9$, which corresponds to striped ground states of width $h = 8$. We see that the specific heat has a sharp peak at a temperature $T_{C2} \equiv T \cong 5g$, followed by a broad peak at the temperature $T_{C1} \equiv T \cong 10g$. We believe that the sharp peak at T_{C2} corresponds to the breakup of the striped phase into a phase consisting of extended domains (tetragonal phase). This transition

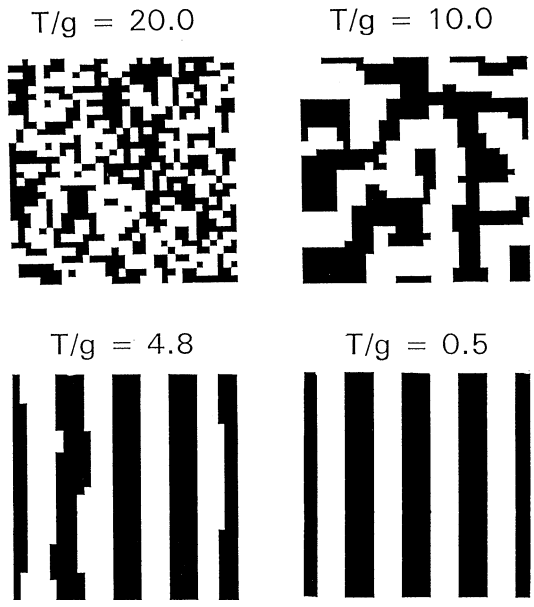

Fig. 1. The evolution of the system during simulated annealing from the high temperature (paramagnetic) phase to the ground (striped) phase.

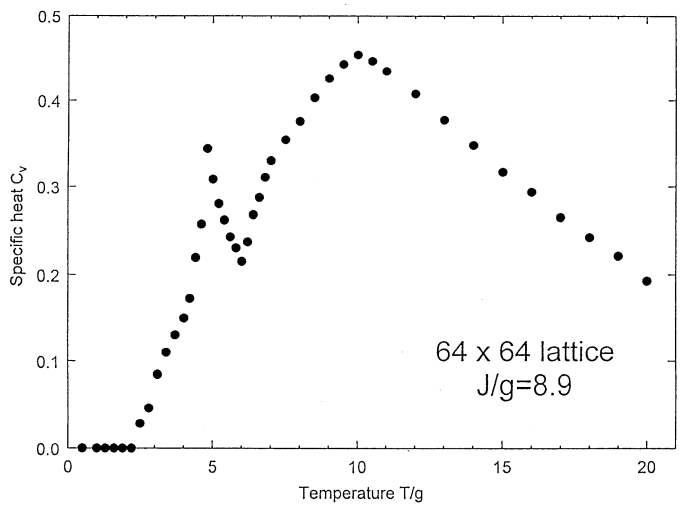

Fig. 2. Specific heat versus temperature for $J/g = 8.9$ ($h = 8$).

is associated with a loss of the translational and orientational orders encountered in the striped phase and it can be defined with the disappearance of the order parameter defined below. This transition is seemingly of the first-order, while the second peak at T_{C1} is associated with the breakup of the extended domains into the

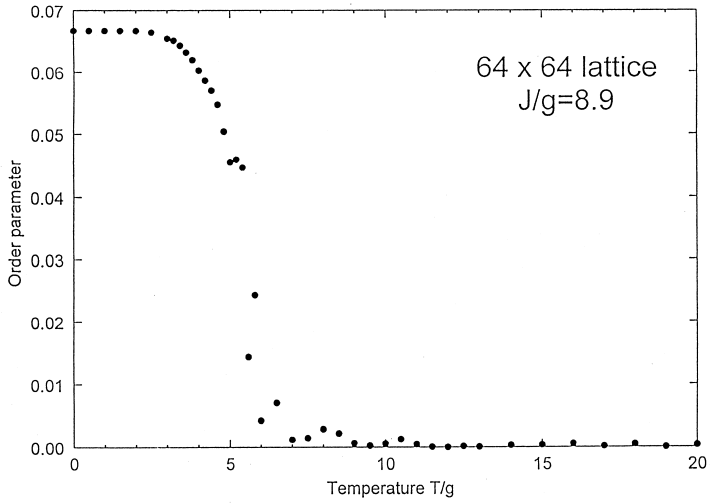

Fig. 3. Order parameter versus temperature. The drop corresponds to a continuous phase transition from the striped phase to a phase with no net orientation.

fully disordered (paramagnetic) phase. This transition is likely of the second-order. The broad bulk behaviour in the specific heat is anticipated as a Schottky anomaly for an Ising-$\frac{1}{2}$ system.

In order to identify the orientational symmetry of the striped state, we define the domain order parameter

$$\eta = \frac{1}{N} \left\langle \left| \sum_j \left| \sum_i S_{ij} \right| - \sum_i \left| \sum_j S_{ij} \right| \right| \right\rangle , \tag{2}$$

where $N = L \times L$ is the number of spins and $\langle \ldots \rangle$ stands for thermal average. For the fully striped phase, $\eta = 1$. This order parameter is plotted as a function of temperature in Fig. 3 for $J/g = 8.9$. This plot provides a signature of a continuous phase transition from the striped phase to the orientationally disordered phase at $T/g \cong 5$, even though there is not enough evidence to rule out the case of a first-order transition, motivated from the sharpness of the spin structure. In conclusion, the transition appears to result in a complete loss of orientational and translational orders, while the transition temperature exhibits a nontrivial dependence on the strength of the exchange interaction J. Still, further calculations are needed to resolve the nature of this transition.

As we have discussed previously, the system exhibits two order-disorder phase transitions. In order to get better understanding of the first phase transition, we looked at the values of the local magnetic field, defined as

$$h_i = J \sum_j S_j - g \sum_j \frac{S_j}{r_{ij}^3} , \tag{3}$$

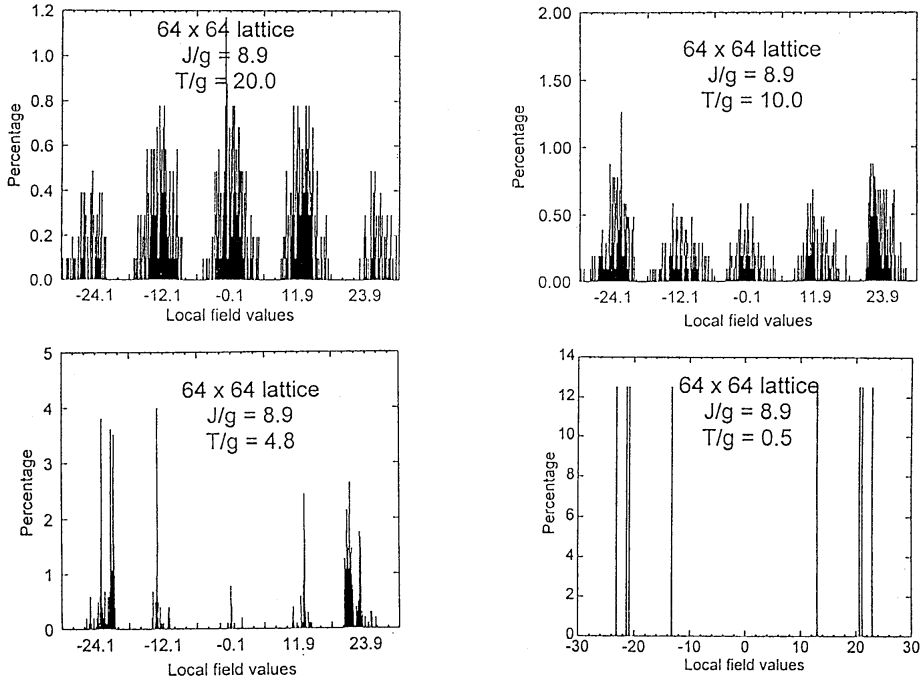

Fig. 4. A sequence of the distribution of the local magnetic field. The temperatures and configurations chosen are those of Fig. 1.

where the first sum is restricted to nearest-neighbors, and the second is taken over the whole lattice. In Fig. 4 we show the distribution of the local magnetic field for the configurations shown in Fig. 1. The local field for the paramagnetic phase has five Gaussian-like peaks, which correspond to the five possible configurations: all four neighbors parallel, three parallel and one antiparallel, two parallel and two antiparallel, one parallel and three antiparallel, and all four neighboring spins antiparallel to the central spin. The central peak (corresponding to the spins with two neighbors parallel and two antiparallel to them) is higher for high temperatures, reflecting the fact that the configuration is disordered, but its relative weight gets smaller as the temperature decreases. Below the transition point $T_{C1} \cong 10g$, where a transition from the paramagnetic phase to the extended domains phase occurs, this peak becomes lower than the remaining four, and keeps getting lower as the temperature is decreased. Near the transition point $T_{C2} \cong 5g$ (striped phase-extended domains phase), this peak almost disappears, which reflects the fact that there are already very few spins with two neighbors aligned parallel and two neighbors aligned antiparallel to them. The local magnetic field configuration remains practically the same as the temperature decreases, until we get to $T < T_{C2}$. We believe this is due to the fact that the fluctuations in the domain walls are still strong enough and the system has not reached the striped configuration yet. Then,

just below T_{C2}, the configuration of the local magnetic field changes into the one characteristic for the striped phase; eight distinct spikes are present, four of them corresponding to the four non-equivalent positions of spins within the "up-spin" stripe and four to the respective positions of spins within the "down-spin" stripe. Of course, all spikes have the same weight and the configuration of the local field remains the same until the temperature reaches zero.

As we argued previously, the transition at T_{C2} from the striped phase to the extended domains phase is due to the loss of translational and orientational order associated with the striped phase. Next, we focused our attention on the broad peak in the specific heat at T_{C1}, which corresponds to the transition from the disordered (paramagnetic) phase to the extended domains phase. For a better understanding of what is happening with the system, we calculated the specific heat from the values of the local field. In the first order of approximation, we calculated the specific heat from the energy cost to flip one spin, in the field created by the rest of the lattice. That energy cost will be $-2h_iS_i$, where h_i is the local field. Then the specific heat can be calculated as in the two-level system. We did the calculations for a 16×16 lattice and a 32×32 lattice at $J/g = 8.9$, averaging each measurement over ten different spin configurations for each temperature. The variation of specific heat versus the temperature is given in Fig. 5. We notice that the temperature-dependence of the specific heat in the first order of approximation exhibits a peak around $T \cong 10g$, but the peak is barely discernible, and the values of the specific heat obtained from the local field are much lower than those obtained from the Monte Carlo simulations (around 25%).

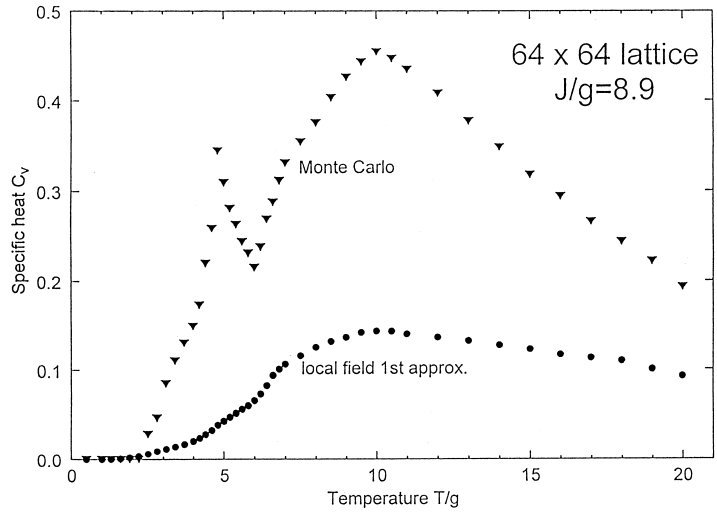

Fig. 5. Specific heat calculated from the values of the local magnetic field, in the first order of approximation. The values obtained from Monte Carlo simulations are shown for comparison. The peak is barely discernible and the height is far from the "true" value.

In the second order of approximation, we considered a pair of spins in the field of the remaining spins. Starting from the actual configuration, we calculate the energy cost to flip one spin ($-2h_1S_1$), then the energy cost to flip the other spin ($-2h_2S_2$), and then both spins ($-2h_1S_1 - 2h_2S_2 + 4J_{12}S_1S_2$, where $J_{12} = -J + g/r_{12}^3$). We have to calculate the specific heat for a four-level system, with energy levels E_0, $E_0 - 2h_1S_1$, $E_0 - 2h_2S_2$, $E_0 - 2h_1S_1 - 2h_2S_2 + 4J_{12}S_1S_2$.

We did the calculations for the 16×16 lattice and the 32×32 lattice at $J/g = 8.9$, again averaging each measurement over ten different spin configurations for each temperature. The temperature dependence of the specific heat is shown in the Fig. 6. From the second order of approximation, we again find the peak at $T \cong 10g$. The values of the specific heat at the peak have already reached around 65% of those obtained from Monte Carlo simulations and the peak is more expressed than the peak we get in the first order of approximation. We believe this reflects the fact that the spin correlation is very strong, so the effects are collective, rather than individual.

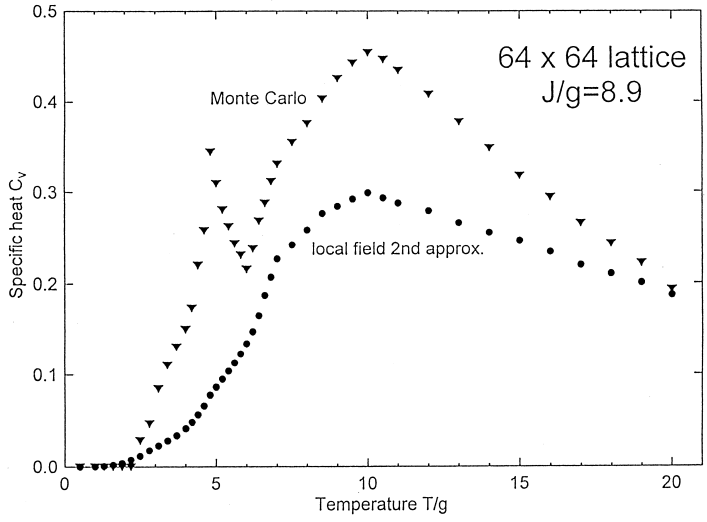

Fig. 6. Specific heat calculated from the values of the local magnetic field, in the second order of approximation. The peak is quite pronounced, and the height has already reached around 65% of the value obtained from Monte Carlo simulations.

3. Conclusions

In conclusion, we have obtained the phase structure of a two-dimensional Ising spin system with competing short range exchange and long range dipolar interactions. We have numerically calculated the specific heat, and the distribution of the local magnetic fields. The sharp peak in the specific heat is due to the loss of translational and orientational order associated with the striped phase. The broad peak in the

specific heat is due to the transition from the extended domain phase to a fully disordered (paramagnetic) phase. The specific heat calculated with the use of the local magnetic fields also gives a broad maximum, in agreement with Monte Carlo simulations.

In this work, we gave evidence of a two-step character of the disordering in a dipolar Ising ferromagnet, but we have not excluded any extra phases, which might be sustained by the present model, as for example the "rotational domain walls," or a reorientation transition to an in-plane magnetization discussed in Ref. 14. The reorientation transition is feasible in sufficiently thick films, which is not undertaken in the present model. The phase diagram predicted by the present model has been observed in a series of experiments in ultrathin magnetic films, as in Fe/Cu(100).[9]

Acknowledgment

Ames Laboratory is operated for the U.S. Department of Energy by Iowa State University under contract No. W-7405-Eng-82.

References

1. T. Garel and S. Doniach, *Phys. Rev.* **B26**, 325 (1982).
2. Y. Yafet and E. M. Gyorgy, *Phys. Rev.* **B38**, 9145 (1988).
3. B. Kaplan and G. A. Gehring, *J. Magn. Magn. Mater.* **128**, 111 (1993).
4. M. B. Taylor and B. L. Gyorffy, *J. Phys. Condens. Matter* **5**, 4527 (1993).
5. A. B. MacIsaac, J. P. Whitehead, M. C. Robinson and K. De'Bell, *Phys. Rev.* **B51**, 16033 (1995).
6. I. Booth, A. B. MacIsaac, J. P. Whitehead and K. De'Bell, *Phys. Rev. Lett.* **75**, 950 (1995).
7. M. Seul and R. Wolfe, *Phys. Rev. Lett.* **68**, 2460 (1992).
8. J. Lindner, P. Poulopoulos, F. Wilhelm, M. Farle and K. Baberschke, *Phys. Rev.* **B62**, 10431 (2000).
9. E. Mentz, A. Bauer, T. Günther and G. Kaindl, *Phys. Rev.* **60**, 7379 (1999); R. Allenspach and A. Bischof, *Phys. Rev. Lett.* **69**, 3385 (1992); D. P. Pappas, K.-P. Kämper and H. Hopster, *ibid.* **64**, 3179 (1990); A. Berger, F. Feldmann, H. Zillgen and M. Wuttig, *J. Magn. Magn. Mater.* **183**, 35 (1998); Li Dongqi, M. Freitag, J. Pearson, Z. Q. Qiu and S. D. Bader, *J. Appl. Phys.* **76**, 6425 (1994); J. Thomassen, F. May, B. Feldmann, M. Wuttig and H. Ibach, *Phys. Rev. Lett.* **69**, 3831 (1992); A. Vaterlaus, C. Stamm, U. Maier, M. G. Pini, P. Politi and D. Pescia, *ibid.* **84**, 2247 (2000).
10. R. Allenspach, M. Stampanoni and A. Bischof, *Phys. Rev. Lett.* **65**, 3344 (1990); M. Dreyer, M. Kleiber, A. Wadas and R. Wiesendanger, *Phys. Rev.* **B59**, 4273 (1999).
11. R. Czech and J. Villain, *J. Phys. Condens. Matter* **1**, 619 (1989).
12. A. Kashuba and V. L. Pokrovsky, *Phys. Rev. Lett.* **70**, 3155 (1993).
13. G. A. Gehring and M. Keskin, *J. Phys. Condens. Matter* **5**, L581 (1993).
14. Ar. Abanov, V. Kalatsky, V. L. Pokrovsky and W. M. Saslow, *Phys. Rev.* **B51**, 1023 (1995).